Simulation of Cold Forging Processes using a Mixed Isotropic-Kinematik Hardening Model

Lander Galdos[1, a)], Julen Agirre[1, b)], Nagore Otegi[1, c)], Joseba Mendiguren[1, d)] and Eneko Saenz de Argandoña[1, e)]

[1]Advanced Material Forming Processes research group, Mondragon Unibertsitatea, Loramendi 4, 20500 Arrasate-Mondragon, Spain

[a)] Corresponding author: lgaldos@mondragon.edu
[b)] jagirreb@mondragon.edu
[c)] notegi@mondragon.edu
[d)] jmendiguren@mondragon.edu
[e)] esaenzdeargan@mondragon.edu

Abstract. Cold forging is a manufacturing process where a bar stock is inserted into a die and squeezed with a second closed die. It is one of the most widely used chipless forming processes, often requiring no machining or additional operations to get tight tolerances. Because materials to be formed are increasingly harder and the geometrical complexity is greater, the finite element simulation is becoming an essential tool for process design. This study proposes the use of the Chaboche hardening model for the cold forging simulation of a 42CrMoS4Al material industrial automotive ball pin. The material model has been fitted with experimental data obtained from cyclic torsion tests at different reversal plastic strains as well as monotonic torsion tests at different strain rates. Comparison between the classical isotropic hardening and the new mixed hardening model are presented for the different forging steps.

Keywords: Cold forging, Numerical simulation, Mixed hardening

1. Introduction

The cold forging is a bulk forming process that aims to obtain near net shape semi-finished components. Unlike the hot forging, the cold forging process produces very precise components having tight geometrical tolerances and good surface finishing. Usually small to medium components are produced by this technology using high production rate horizontal presses. Typical components are bolts, geared shafts and pins among others [1, 2].

Like in many metal-forming processes, cold forging industry is increasingly using the finite element modelling for process and tool design. In this regard, the numerical modelling is becoming state of the art in the cold forging companies and usual outputs are the material flow, used for checking the die filling and folds, and the punch forces. Advanced features that are not fully stablished in the sector are the advanced fracture criteria as proposed by Bariani et al. and Stebunov et al. [3,4] and the analysis of the resulting residual stresses and their influence on the final properties [5,6].

Because the accuracy level demanded to the numerical models is high during cold forged process definition, take into account that geometrical accuracy is often cents of millimeter, the accuracy of numerical inputs is of high importance. Regardless the mesh quality, the remeshing strategy and the numerical method used to solve the problem, the material and contact definition are critical for getting the desired reliability. Latest works for properly identifying the friction coefficient for cold forging simulation have being led by the "Lubrication" Subgroup of the International Cold Forging Group (ICFG). An inter-laboratory comparison using different friction tests was done by different re-known authors and conclusions were presented in [7]. Regarding the material modelling, Bruschi et al. presented a deep review about the modelling of material behaviour in sheet metal forming [8]. In the paper, relevant hardening models for capturing metals Bauschinger effect are explained. The use of mixed isotropic and kinematic hardening models influence the final accuracy of the numerical models, especially in terms of springback and residual stresses. These hardening models have been rarely employed in the cold forging process simulations.

For this reason, the main objective of this paper is to show the influence the hardening model has on the numerical results of an industrial automotive ball pin forging. The state of the art for cyclic behavior modelling and cyclic material characterization is presented and experimental results obtained by using cyclic torsion tests are presented and discussed by the authors for a cold forging steel.

The Chaboche and Lemaitre mixed hardening model is presented and the material parameters identification procedure is explained using the experimental data obtained in the cyclic torsion tests. Finally, the numerical results obtained using an isotropic hardening material model and the fitted mixed hardening model are shown and compared by using an industrially often-used FEM software.

2. Material cyclic characterization

2.1. Material properties

The 42CrMoS4Al case hardening steel used to produce automotive ball pins was selected for the current study. 26 mm diameter steel rods were used for the experimental testing. The material was obtained in the annealed condition, which is the as-received state used in the forging companies for producing the selected component. Material composition is shown in table 1.

Table 1. Chemical composition of 42CrMoS4Al case hardening steel.

C	Mn	Si	P	S	Cr	Mo	Cu	Al
0.42	0.76	0.14	0.009	0.025	1.03	0.176	0.14	0.024

The as received material microstructure is shown in figure 1. The edging used for revealing the microstructure was the Nital-Beraha. Ferrite is colored in white, the Martensite is dark brown and Bainite is light brown.

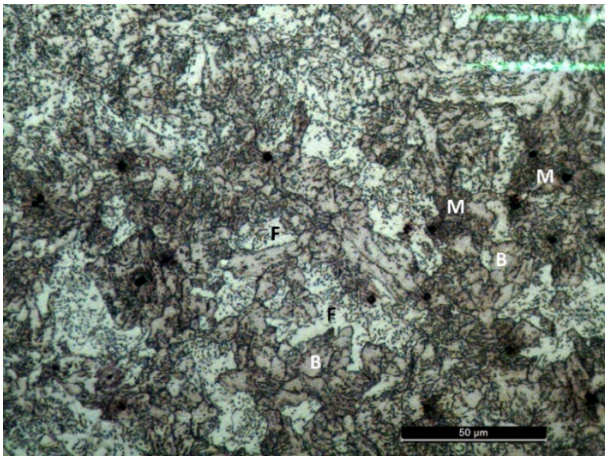

Figure 1. As received microstructure of 42CrMoS4Al case hardening steel.

2.2. Monotonic and cyclic material testing. State of the art

In metal forming operations and cold forging processes, the metals are normally subjected to very complex strain paths that include loading reversal. For this reason, complex phenomenological hardening models are increasingly being introduced in finite element modelling codes to provide accurate predictions of material behavior. Four types of hardening may arise during forming processes: (i) isotropic hardening, which refers to the proportional expansion of the initial yield surface; (ii) kinematic hardening, if the deforming material shows a yield surface that does not change in form and size, but translates in the stress space; (iii) rotational hardening, which causes the yield locus to rotate; (iv) distortional hardening, which causes the yield locus to distort [8].

Mixed isotropic and kinematic hardening models are becoming of common use in the sheet metal forming simulations since they significantly influence the springback prediction accuracy and are able to reproduce different phenomenon such as the Bauschinger effect, the transient behaviour, the permanent softening and ratcheting [9-11]. The different phenomenon that appear during the reverse loading are illustrated in figure 2.

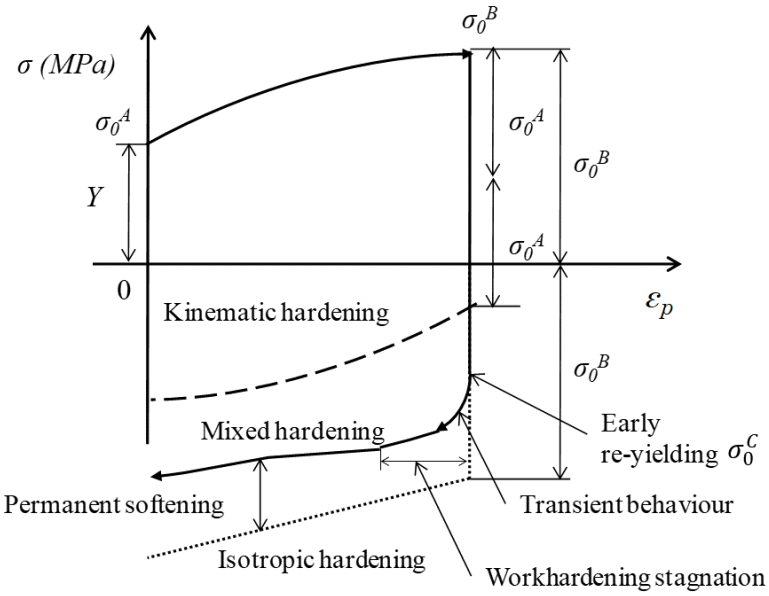

Figure 2. As received microstructure of 42CrMoS4Al case hardening steel.

Different authors have proposed several reverse loading tests needed for the cyclic characterization of sheet metals and the analysis of these phenomena. Experimental data using a tension–compression test were obtained for different materials by Silvestre et al. [12]. The test was valid for plastic strain levels up to ±3%. Brunet et al. [13] identified the hardening parameters by using bending tests of a mild steel. The results showed some limitations and uncertainties due to the fact that the strain state in the sample was not exactly a pure strain state of bending. The cyclic three point bending test was also used to determine various hardening laws of DP600 and 220 IF steels by Eggertsen and Mattiasson [14].

Other authors combined different tests, such as Weiss et al. [15], who used bending and simple shear tests for studying the Bauschinger effect of various DP steel grades at high strain levels. Miyauchi et al. presented a very interesting test for cyclic shear testing of metal sheets [16] and Tekkaya et al. extended the in plane torsion test for the characterization of sheet metals at very high strain levels [17].

The above-mentioned works show that the sheet metal forming community is well advanced in the cyclic characterization of materials. Many authors used tension-compression tests for the characterization of the kinematic behaviour of solid samples at very low strain levels with the aim to be used in fatigue modelling. However, very few works intended for forming process modelling of bulk material were found during the literature review. Madej et al. used tension-compression tests of solid samples cut from thick sheets for the study of the high temperature levelling of thick plates [18]. Strain levels were small compared to cold forging. Narita et al. used small size shear samples cut from wire to study the influence of the hardening model in the springback prediction of cold forged extruded components [19-21]. Strains up to 35% were achieved before strain reversal and the Yoshida-Uemori model was used in their works for the cyclic behaviour modelling of the initial wires. The estimated final extruded diameter by the Yoshida-Uemori model was more uniform and closer to the experimental results.

Finally, it is worth to mention that torsion tests of solid samples are suitable for high strain level testing of metallic materials. In this regard, Badiola et al. used this experimental procedure to study the cyclic behavior of rods and understand the austenite–ferrite phase transformation in a Nb-microalloyed steel at high temperature [22]. Her et al. recently presented a new method to obtain high strain flow curves for cold forging including kinematic hardening by using a combination of extrusion plus tensile or compression tests [23].

2.3. Cyclic torsion tests

Cyclic torsion tests were used for the kinematic characterization of the material at strain levels similar to the ones reached during cold forging. It is well known that torsion tests are capable to reach very high

strains due to the stress state that is present in the material during the test as it was mentioned before. The geometry of the sample and the torsion tester are shown in figure 3.

Cyclic tests were performed using three different reversal angles: 100º, 200º and 300º (approximate equivalent total strains of 0.25, 0.5 and 0.75). After clockwise twisting of the samples up to the desired reversal angle the rotation direction was inversed and the material was twist counterclockwise until rupture occurred. The elastic part of the cyclic curves was removed using the 0.2% offset method, which is equal to approximately 1º offset. Finally the torque–twist angle data was converted into shear stress–shear strain according to the method proposed by Fields and Backofen [24] and then, into true stress–true strain by applying the Von Mises criterion. The experimental stress–strain curves are shown in figure 4.

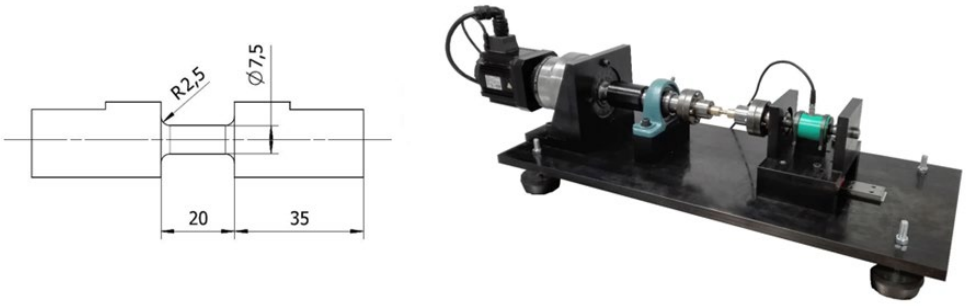

Figure 3. Torsion sample dimensions and Torsion test bench.

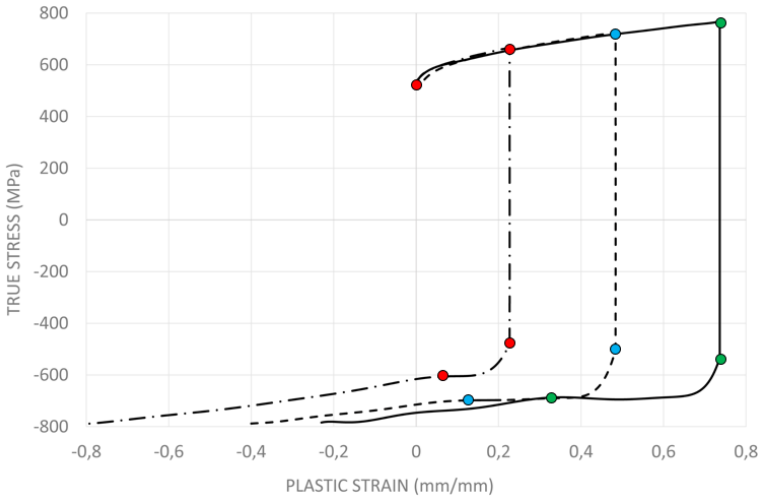

Figure 4. Experimental stress-strain curves at different reversal angles.

2.4. Evolution of the kinematic behavior of the analyzed steel

The analysis of the cyclic experimental curves was performed to understand the kinematic behavior of the selected steel. The evolution of the tension and compression yield stress ratio (σ_0^B/σ_0^C) was analysed for the different cyclic reversals. As it is shown in figure 5 the Bauschinger effect reaches an asymptotic value after an initial decrease and thus, the isotropic hardening or yield surface expansion suffered by the material is continuously compensated in the same ratio by the kinematic hardening or the translation of the yield surface. The evolution of the transient softening and the work hardening stagnation is shown in figure 6. The definition of the measured lengths for both variables are detailed in figure 1. The transient softening length or strain is almost constant for all the cyclic reversals while the work hardening stagnation increases with the applied prestrain. This is a well-known phenomena for stress reversal at large strains. Transmission Electron Microscope observations revealed the main features of the evolution of dislocation substructures under stress reversal. During the strain-hardening stagnation, preformed dislocation walls gradually disintegrate. The amount of reverse strain which is necessary for the complete dissolution of these walls increases with the prestrain [25].

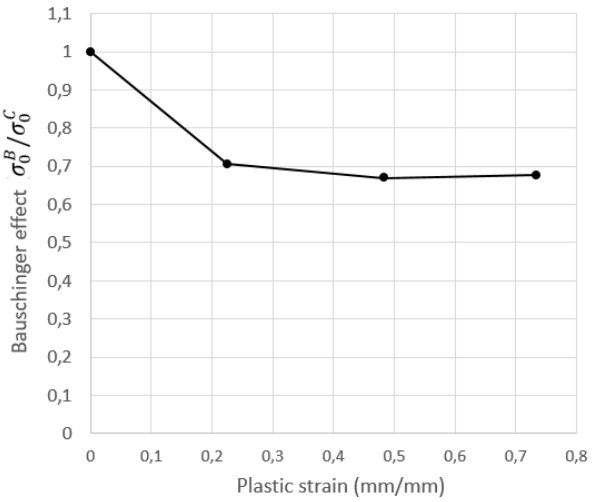

Figure 5. Evolution of Bauschinger ratio.

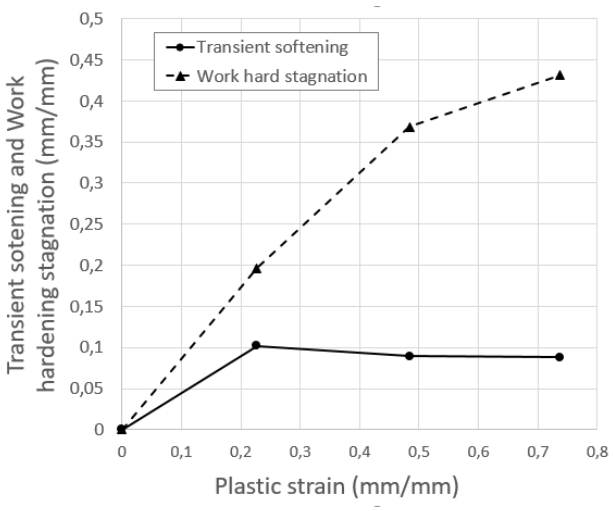

Figure 6. Evolution of transient softening and stagnation behaviour.

Finally, the evolution of the isotropic hardening and the kinematic hardening have been analyzed. From figure 7 and for the uniaxial cyclic loading case the values of the isotropic hardening R and the kinematic hardening X can be calculated analytically for the different reversal strains as follows:

$$R = \left(\frac{\sigma_0^B - \sigma_0^C}{2}\right) - \sigma_0^A \qquad (1)$$

$$X = \sigma_0^B - (\sigma_0^A + R) = \frac{\sigma_0^B + \sigma_0^C}{2} \qquad (2)$$

Note that σ_0^C is negative in the formulae, as it is the compression yield stress of the material after loading. $\sigma_0^A$and $\sigma_0^B$are positive being the initial yield stress and yield stress after uniaxial pre-straining.. The evolution of isotropic hardening (R) and the kinematic hardening (X) for the different cyclic tests is shown in figure 8. As it is observed, the R follows a linear evolution while X tends to stabilize at a plastic strain of approximately 0.8.

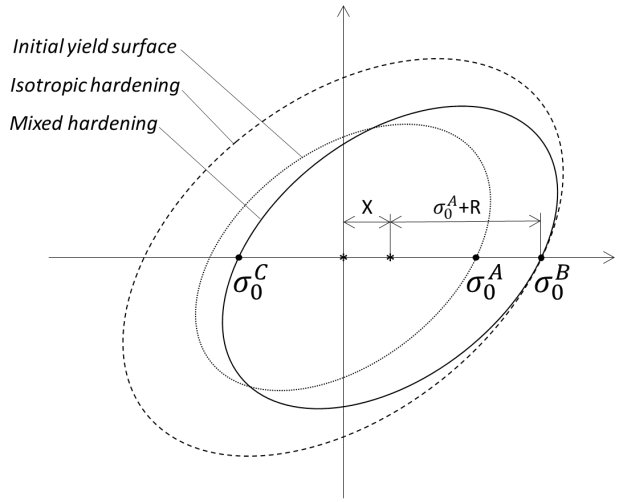

Figure 7. Representation of isotropic and kinematic hardening.

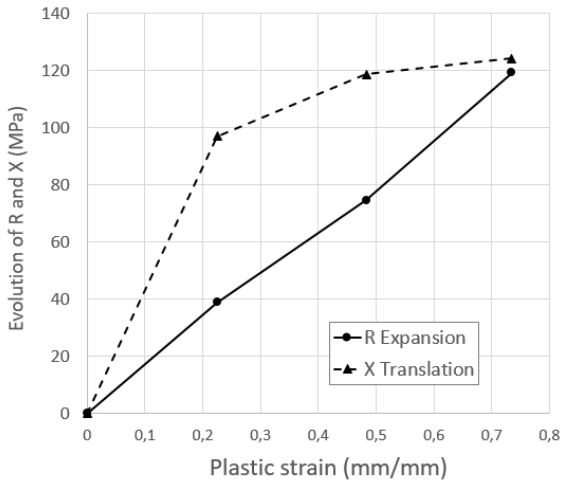

Figure 8. Evolution of isotropic and kinematic hardening.

3. Parameter identification of mixed Chaboche and Lemaitre model

The Chaboche and Lemaitre hardening model (1990) [26] was combined with the Von Mises yield criteria, as these are recommended for cyclic plasticity analyses and widely distributed in commercial FE-codes. The Von Mises yield criteria can be expressed:

The Chaboche and Lemaitre hardening model (1990) [25] was combined with the Von Mises yield criteria, as these are recommended for cyclic plasticity analyses and widely distributed in commercial FE-codes. The Von Mises yield criteria can be expressed:

$$\phi(\boldsymbol{\sigma}, \boldsymbol{X}, \sigma_y) = \sqrt{{}^3/_2\,(\boldsymbol{\sigma} - \boldsymbol{X}) : (\boldsymbol{\sigma} - \boldsymbol{X})} - \sigma_y - R \qquad (3)$$

where $\boldsymbol{\sigma}$ denotes the deviatoric stress tensor, $\boldsymbol{X}$ is the deviatoric backstress tensor, σ_y is the initial yield stress and R is the isotropic hardening. An associated flow rule has been considered to define the plastic strain increment.

The Chaboche and Lemaitre hardening model is a mixed isotropic-kinematic hardening formulation. The nonlinear kinematic hardening describes the movement of the yield surface by means of the evolution of the backstress. The change in the size of the yield surface, is related to the isotropic hardening and is introduced by means of the initial value of the yield strength σ_y and the isotropic variable R. In the proposed model, the evolution of the isotropic hardening is defined in function of the accumulated plastic strain $\mathrm{d}\bar{\varepsilon_p}$ by the following law:

$$\mathrm{d}R = b \cdot (Q - R) \cdot \mathrm{d}\bar{\varepsilon}p \qquad (4)$$

where Q and b are material parameters of the model. The kinematic evolution of the yield surface, proposed by Chaboche et al. is presented in Eq. (5). This model is based on a decomposition of the non-linear kinematic hardening rule proposed by Armstrong and Frederik (1966). Chaboche decomposed a stable hysteresis curve in several parts and it was observed that increasing the material parameters of the hardening rule by the superposition of backstresses, a more accurate model was obtained [16]. However, in this work only one backstress has been considered in the model definition.

$$d\boldsymbol{X} = \frac{2}{3} \cdot C \cdot d\boldsymbol{\varepsilon}_p - \gamma \boldsymbol{X} \cdot \mathrm{d}\bar{\varepsilon_p} \qquad (5)$$

where C and γ are the material parameters to be fitted.

The parameter identification method consisted of an unconstrained non-linear optimization proposed by Nelder and Mead [51] available at Matlab®. First, initial values of Q, b, C and γ where found using the data of figure 8. After these first calculation the error function shown in Eq. (6) was minimized using all the experimental data of the three cyclic tests.

$$f_{obj} = \frac{1}{n} \sum_{i=1}^{n} \left| \sigma_i^{exp} - \sigma_i^{model} \right| \qquad (6)$$

The results of the fitting are presented in figure 9. The model taking into account only the isotropic hardening was labelled as IH while the mixed isotropic and kinematic model with one backstress is labelled as KH. As can be observed, the model was able to predict the cyclic hardening of the material. The model predicted the Bauschinger Effect observed in the experimental results. However, was not able to accurately predict the transient behavior and work hardening stagnation. This can be explained because only one backstress tensor was used in this study and at least two are needed for capturing the transient behavior. The four material parameters involved in the model obtained by means of the explained optimization method are presented in table 2.

Table 2. Material parameters of the mixed Chaboche and Lemaitre hardening model.

Isoropic model IH			Mixed hardening model IK			
σ_0	Q	b	Q	b	C	γ
525 MPa	335 MPa	1.45	300 MPa	0.5	850	7.0

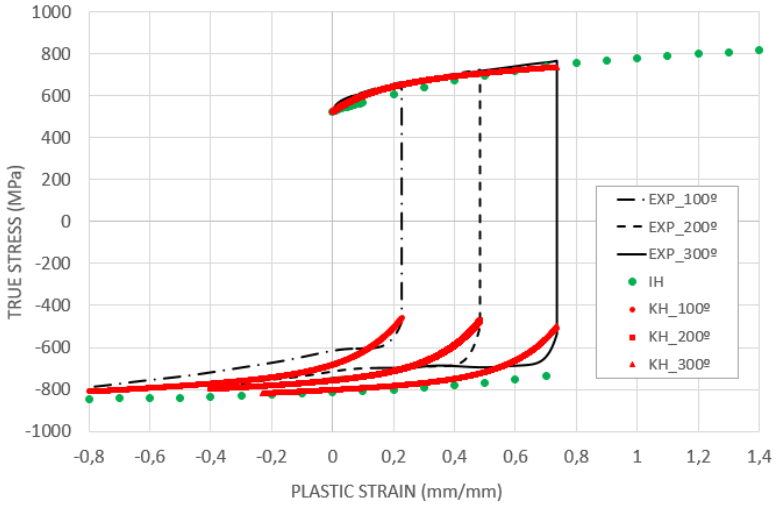

Figure 9. Fitting of Chaboche and Lemaitre model to experimental curves.

4. Finite Element Modelling of a ball pin cold forging

In order to quantify the influence the hardening model has on the numerical results, a real cold forging process of a ball pin was simulated. For confidential issues, only the first three operations were simulated; one upsetting, one extrusion operation and the forging of the ball.

FORGE® NxT was used for the process modelling. A full 3D model was used although the model is asymmetric because the material model was coded for a 3D general case. One twelfth of the billet was simulated using two symmetry planes to avoid excessive computing time. The mesh sensitivity analysis suggested the use of 0.5 mm mesh size in the most strained areas, the transition and rounded zones. For this reason, the billet was meshed using tetrahedral elements with a general mesh size of 1.5 mm and remeshing boxes of 0.5 mm in the transition zones. A friction value of μ=0.05 was used in the simulations as suggested in [7]. Simulations were run with the two material models, a pure isotropic model and a mixed kinematic hardening model as explained before. For the numerical comparison the material flow, the equivalent Von Mises stress after each process step, the residual stresses after punch-die release and the punch forces were compared.

The material flow analysis, displacement in Z direction, (see figure 10) demonstrates that material flow is similar in both material models. The equivalent strain analysis shows similar results and strain levels are similar for both material models. This can be explained because the closed die forging is driven by the die and punch geometries. The material displacement after punch release is higher for the isotropic model. This can be explained because higher residual stresses result when using a isotropic model in the lower part of the ball pin.

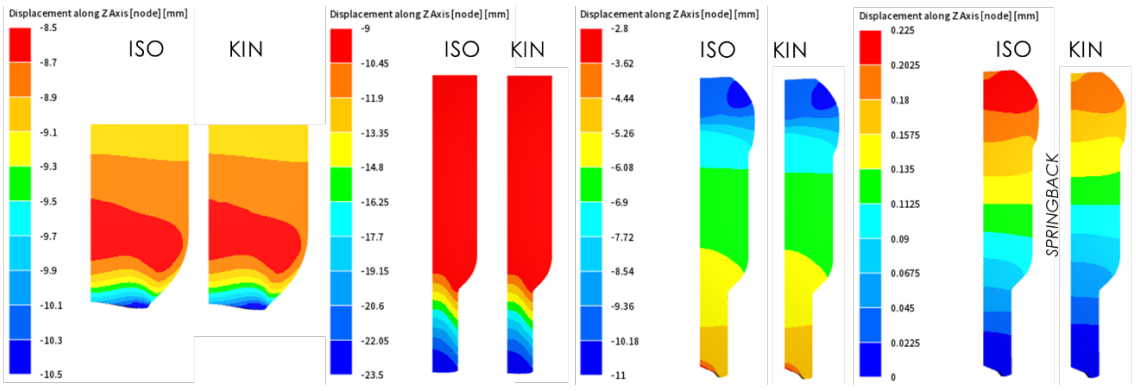

Figure 10. Material flow results (displacement in Z direction). Upsetting, Extrusion and Ball forging operations together with the final springback.

The equivalent Von Mises stresses after each process step are shown in figure 11. The Upsetting and Extrusion operations show similar stress levels for both models. However, the third operation clearly shows that the compression of the lower part after the extrusion operation is highly affected by the hardening model. AT 50% of the punch stroke, when the bottom part of the ball pin is forged, shows significantly higher stress levels for the isotropic model than the kinematic one. This is also observed after the punch reaches the 100% of the stroke at this operation and this explains the higher springback observed after this forging operation in the material flow results.

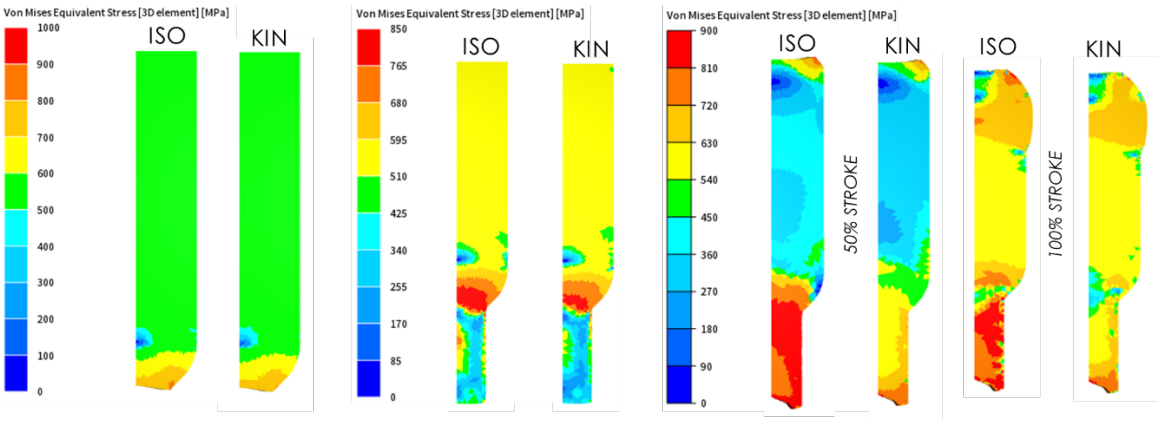

Figure 11. Material flow results (displacement in Z direction). Upsetting, Extrusion and Ball forging operations together with the final springback.

Finally, punch forces for the different hardening models and operations are shown in figure 12. Kinematic model forces are lower than the isotropic model. This is observed principally in the extrusion operation. The difference is not remarkable in the last operation where the kinematic hardening model predicts the biggest differences in terms of stresses. However cam be explained because the biggest amount of work is used for the ball forging where the kinematic hardening effect is not important.

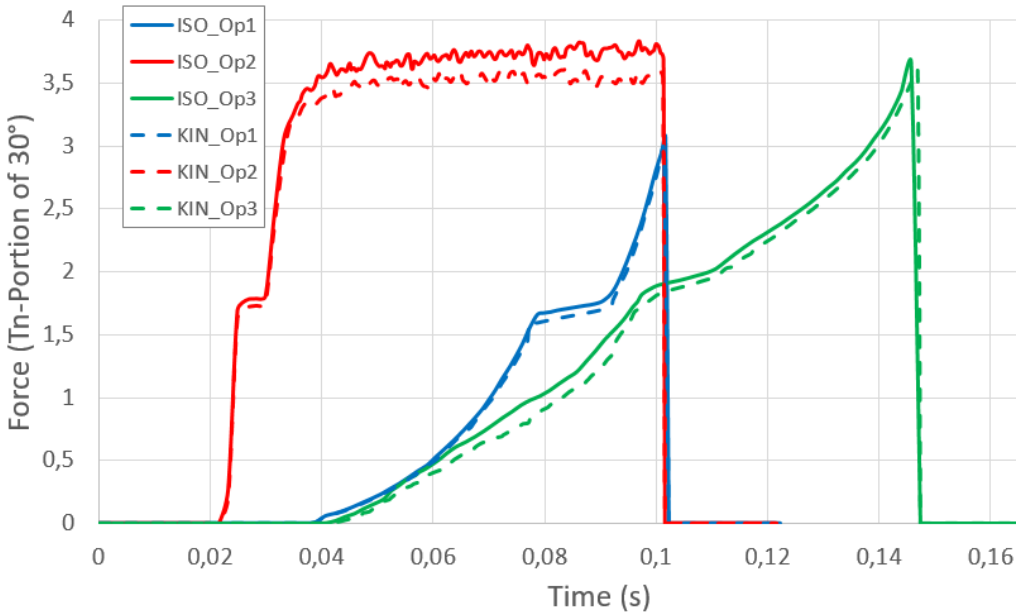

Figure 12. Punch forces for the different hardening models and operations.

5. Conclusions

The 42CrMoS4Al case hardening steel used to produce automotive ball pins was characterized using torsion cyclic tests. The methodology showed the test is suitable for reaching high strain levels and studying the transient softening and work hardening stagnation phenomena. These two effects could be important for the cold forging process modeling because equivalent strains reached in this process are very high.

The experimental results were fitted to the well-known the Chaboche and Lemaitre hardening model. The mixed hardening model was able to capture the Bauschinger effect but the transient softening and work hardening stagnation were not properly captured. The superposition of more backstress tensors needs to be evaluated to enhance the model accuracy. On the other hand the influence of the temperature needs to be also introduced in the model. This is currently being analyzed by the authors.

Different material flow was observed for the kinematic and isotropic models principally in the final springback of the component. Von Mises stresses are different for the two laws during the forging but the biggest influence was observed during the compression after an extrusion operation, where the path change is important. Although the kinematic hardening showed slightly lower punch forces the difference seems to be not relevant for the analyzed component.

6. Acknowledgements

The authors would like to thank the Gipuzkoa Provincial Council for the funding of the RELASHEET research project (Desarrollo de distintos métodos de alivio de tensiones residuales en chapas metálicas) and the Ecenarro S. Coop. cold forging company for their technical support.

References

[1] Sevenler, K., Raghupathi, P. S., & Altan, T. (1987). Forming-sequence design for multistage cold forging. Journal of Mechanical working technology, 14(2), 121-135.
[2] Semiatin, S. L. (2005). ASM Handbook vol. 14A, Metalworking: Bulk Forming. ASM International, Novelty.
[3] Bariani, P. F., Bruschi, S., Ghiotti, A., & Simionato, M. (2011). Ductile fracture prediction in cold forging process chains. CIRP annals, 60(1), 287-290.
[4] Stebunov, S., Vlasov, A., & Biba, N. (2018). Prediction of fracture in cold forging with modified Cockcroft-Latham criterion. Procedia Manufacturing, 15, 519-526.
[5] Gerin, B., Pessard, E., Morel, F., Verdu, C., & Mary, A. (2015). Effect of cold forming on the high cycle fatigue behaviour of a 27MnCr5 steel. Procedia Engineering, 133, 603-612.
[6] Tekkaya, A. E., Allwood, J. M., Bariani, P. F., Bruschi, S., Cao, J., Gramlich, S., ... & Lueg-Althoff, J. (2015). Metal forming beyond shaping: predicting and setting product properties. CIRP Annals, 64(2), 629-653.
[7] Groche, P., Kramer, P., Bay, N., Christiansen, P., Dubar, L., Hayakawa, K., ... & Moreau, P. (2018). Friction coefficients in cold forging: A global perspective. CIRP Annals, 67(1), 261-264.
[8] Bruschi, S., Altan, T., Banabic, D., Bariani, P. F., Brosius, A., Cao, J., ... & Tekkaya, A. E. (2014). Testing and modelling of material behaviour and formability in sheet metal forming. CIRP Annals, 63(2), 727-749.
[9] Lee, M. G., Kim, D., Kim, C., Wenner, M. L., & Chung, K. (2005). Spring-back evaluation of automotive sheets based on isotropic–kinematic hardening laws and non-quadratic anisotropic yield functions, part III: applications. International journal of plasticity, 21(5), 915-953.
[10] Taherizadeh, A., Green, D. E., Ghaei, A., & Yoon, J. W. (2010). A non-associated constitutive model with mixed iso-kinematic hardening for finite element simulation of sheet metal forming. International journal of plasticity, 26(2), 288-309.
[11] Vladimirov, I. N., Pietryga, M. P., & Reese, S. (2010). Anisotropic finite elastoplasticity with nonlinear kinematic and isotropic hardening and application to sheet metal forming. International Journal of Plasticity, 26(5), 659-687.
[12] Silvestre, E., Mendiguren, J., Galdos, L., & De Argandoña, E. S. (2015). Comparison of the hardening behaviour of different steel families: From mild and stainless steel to advanced high strength steels. International journal of mechanical sciences, 101, 10-20.

[13] Brunet, M., Morestin, F., & Godereaux, S. (2001). Nonlinear kinematic hardening identification for anisotropic sheet metals with bending-unbending tests. Journal of Engineering Materials and Technology, 123(4), 378-383.
[14] Eggertsen, P. A., & Mattiasson, K. (2010). An efficient inverse approach for material hardening parameter identification from a three-point bending test. Engineering with Computers, 26(2), 159-170.
[15] Weiss, M., Kupke, A., Manach, P. Y., Galdos, L., & Hodgson, P. D. (2015). On the Bauschinger effect in dual phase steel at high levels of strain. Materials Science and Engineering: A, 643, 127-136.
[16] Miyauchi, K. (1984). Stress--Strain Relationship in Simple Shear of In-Plane Deformation for Various Steel Sheets. In Efficiency in Sheet Metal Forming, IDDRG 13 th Biennial Congress (pp. 360-371).
[17] Yin, Q., Tekkaya, A. E., & Traphöner, H. (2015). Determining cyclic flow curves using the in-plane torsion test. CIRP Annals, 64(1), 261-264.
[18] Madej, L., Muszka, K., Perzyński, K., Majta, J., & Pietrzyk, M. (2011). Computer aided development of the levelling technology for flat products. CIRP annals, 60(1), 291-294.
[19] Narita, S., Uemori, T., Hayakawa, K., & Kubota, Y. (2016). Effect of hardening rule on analysis of forming and strength of multistage cold forged bolt without heat treatment. J. Jpn. Soc. Technol. Plast, 54-670.
[20] Narita, S., Hayakawa, K., Kubota, Y., Harada, T., & Uemori, T. (2017). Effect of hardening rule for spring back behavior of forging. Procedia Engineering, 207, 167-172.
[21] Fujii, T., Hayakawa, K., Harada, T., & Narita, S. (2018). Cyclic simple shear test of material for cold forging. Procedia Manufacturing, 15, 1785-1791.
[22] Lanzagorta, J. L., Jorge-Badiola, D., & Gutiérrez, I. (2010). Effect of the strain reversal on austenite–ferrite phase transformation in a Nb-microalloyed steel. Materials Science and Engineering: A, 527(4-5), 934-940.
[23] Hering O., Kolpak F., Dahnke C., Tekkaya E. (2019). High Strain Flow Curves by Mechanical Tests on Specimens Pre-strained by Forward Rod Extrusion, Proceedings of the 52nd ICFG plenary meeting.
[24] D. S. Fields and W. A. Backofen, Determination of strain hardening characteristics by torsion testing, Proc. ASTM Vol. 57 (1957) 1259-1272.
[25] Hu, Z., Rauch, E. F., & Teodosiu, C. (1992). Work-hardening behavior of mild steel under stress reversal at large strains. International Journal of Plasticity, 8(7), 839-856.
[26] J Lemaitre, JL Chaboche, Mechanics of solid materials, Cambridge Univ Pr 1994.